Neurosci Bull April 1, 2011, 27(2): 83–90. http://www.neurosci.cn
DOI: 10.1007/s12264-011-1150-1

·Original Article·

Expression of tyrosine kinase receptor C in the segments of the spinal cord and the cerebral cortex after cord transection in adult rats

Dong-Xiang QIAN[1,2,*], Hong-Tian ZHANG[2,3,*], Ying-Qian CAI[2], Peng LUO[1], Ru-Xiang XU[2,3]

[1]*Department of Neurosurgery, the Third Affiliated Hospital, Guangzhou Medical College, Guangzhou 510150, China*
[2]*Institute of Neurosurgery, Key Laboratory on Brain Function Repair and Regeneration of Guangdong, Southern Medical University, Guangzhou 510282, China*
[3]*Department of Neurosurgery, the Military General Hospital of Beijing PLA, Beijing 100700, China*

Abstract: **Objective** To investigate the role of tyrosine kinase receptor C (TrkC), the receptor of neurotrophin-3 (NT-3), in neuroplasticity following spinal cord injury (SCI). **Methods** Rats with cord transection were allowed to survive for 1, 3, 7 and 14 d post operation (dpo). TrkC expressions at lower thoracic levels of the spinal cord and in precentral gyrus of cerebral cortex were investigated. **Results** TrkC protein levels at both the site of injury (T10–T11) and the neighboring segments (T9 and T12) in the spinal cord decreased significantly at 1-7 dpo, followed by a rapid increase at 14 dpo. The temporal changes in *TrkC* mRNA expression level showed a similar pattern with that of TrkC protein. In addition, the levels of TrkC protein and mRNA at the site of injury (T10–T11) were significantly higher than those at the neighboring spinal segments (T9 and T12). Besides, the levels of TrkC protein and mRNA were higher at the rostral segment than at the caudal segment. However, in the motor cortex, TrkC protein was not detected and *TrkC* mRNA was expressed at a very low level. **Conclusion** These results suggest that TrkC may be involved in neuroplasticity after SCI.

Keywords: tyrosine kinase receptor C; spinal cord injury; plasticity; mRNA

1 Introduction

Although death and functional disability occur frequently after adult spinal cord injury (SCI), spontaneous functional recovery has also been reported to be present[1]. The mechanisms underlying this functional recovery have not been fully understood. It has been widely demonstrated that neurotrophins (NTs) administered to the lesioned spinal cord can promote neuronal regeneration and facilitate functional recovery after SCI[2-4]. However, the roles of endogenous NTs in spinal plasticity and spontaneous functional recovery after SCI are still largely unknown[5].

Among various NTs, neurotrophin-3 (NT-3) which has activity on a broad range of neuron types, has been widely studied[2,6]. NT-3 appears to mediate the trophic activities mainly through activating the tyrosine kinase receptor C (TrkC), although NT-3 can also interact with TrkA and TrkB[7]. Clarifying the roles of endogenous NT-3 and TrkC is helpful in understanding the interaction between NT-3 and TrkC as well as the mechanisms of neuroplasticity. NT-3 protein and mRNA expressions have been detected in the spinal cord following different types of SCI in rodents[8,9]. However, the present knowledge concerning

*These authors contributed equally to this work.
Corresponding author: Ru-Xiang XU
Tel: +86-20-81292171; Fax: +86-20-81202601
E-mail: xuruxiang_neuron@126.com
Article ID:1673-7067(2011)02-0083-08
Received date: 2010-12-13; Accepted date: 2011-02-25

the endogenous expression of TrkC and/or its mRNA in the injured spinal cord is limited and controversial.

The present study aimed to investigate the temporal and spatial changes in TrkC mRNA and protein levels in the spinal cord and the precentral gyrus of cerebral cortex at different time points following cord transection in the adult rats.

2 Materials and methods

2.1 Animals A total number of 50 young adult male Sprague Dawley (SD) rats (weighing 200–250 g) were used in the present study. Animals were housed at standard conditions of humidity and temperature under a 12:12 h light/dark cycle, with free access to food and water. Experiments were carried out in accordance with the guidelines issued by the Committee of Experimental Animals of Southern Medical University. All efforts had been made to minimize animal suffering and to reduce the number of animals used.

2.2 Animal grouping and surgical procedure Animals were randomly divided into 5 groups (n=10 in each group). In group I (the sham-operation group), the rats received laminectomy but with no injury to the spinal cord. These animals were sacrificed at 14 d post operation (dpo). In groups II–V, animals received spinal cord transection operation and were sacrificed at 1, 3, 7 and 14 dpo, respectively. For each operation group, 4 animals were used for immunohistochemical analysis and *in situ* hybridization, 3 for real-time PCR, and 3 for Western blot detection.

The animals were anaesthetized by intraperitoneal injection of 3.6% chloral hydrate. A 2-cm incision was made in the skin of the back, centering at the tenth thoracic vertebra (T10). The supraspinal ligaments were removed, and the spinous processes of T9 and T10 were clipped off with a pair of strong artery forceps, exposing the ligamentum flavum and approximately 1-cm-long spinal cord. After laminectomy at T9–T10 vertebral level, the meningeal membranes were severed, along with the dura mater. The spinal cord was completely transected, and a 2-mm-long region of spinal cord encompassing T8 was removed. The rostral and caudal stumps were lifted after removal of the spinal cord segment, to ensure complete discontinuity. All spinal roots visible in the injury gap were removed, and gelfoam was used for haemostasis. Finally, wound suturing was performed. All the operated animals were allowed to recover spontaneously, without administration of any drug. After transection, the bladder of adult rat was emptied by compression of the abdomen twice per day for at most 3 d until the recovery of micturition reflex.

2.3 Tissue preparation For immunohistochemical analysis, the rats were perfused with 500 mL normal saline via the ascending aorta, followed by 1 L Zamboni's fixative (containing 2% paraformaldehyde and 15% saturated picric acid). The spinal cords and the brain tissues were quickly removed and stored at -80 ^{o}C for immunohistochemical analysis. For RT-PCR and western blot analyses, the cerebral cortex and T9–T12 spinal segments were removed and dissected into approximately 0.5 cm^2 parts on ice, followed by careful removal of the meninges, vessels, spinal roots and dorsal root ganglia. All the samples were stored at -80 ^{o}C until use.

2.4 Immunohistochemistry The immunohistochemical procedure was similar to the previous description[7]. Briefly, sections were transferred to 20% sucrose in 0.1 mol/L PBS. After sinking to the bottom of the container, the tissues were removed, frozen, and sectioned at a thickness of 20 μm with a freezing microtome (CM1900; Leica, Wetzlar, Germany). Each 5 sections were processed for immunohistochemical observation. Free-floating sections were washed 3 times by 0.1 mol/L PBS and then incubated in 0.2% hydrogen peroxide at 37 ^{o}C for 20 min to block the action of any endogenous peroxidase. This was followed by 30-min immersion in PBS containing 0.3% Triton X-100 and 5% normal goat serum at 37 ^{o}C. Afterwards, sections were incubated with mouse anti-TrkC at 4 ^{o}C for 24 h (1: 1 000; Upstate Biotechnology Inc., Lake Placid, NY, USA). Sections were washed for 3 times in 0.1 mol/L PBS, and then incubated with biotinylated anti-rabbit IgG (1:400; Vector Laboratories, CA, USA) for 2 h at 37 ^{o}C. After being washed in 0.1 mol/L PBS for 3 times, sections were incubated with an avidin-biotin-peroxidase reagent (1:100;

ABC Elite, Vector Laboratories, CA, USA), and the immunoreaction products were visualized by incubation in the staining solution containing 0.04% 3,3′-diaminobenzidine, 0.06% nickel sulfate, and 0.06% hydrogen peroxide for 10 min. Sections were mounted, dehydrated, coverslipped, and observed under a light microscope (Olympus, Tokyo, Japan).

To identify the phenotype of TrkC-positive cells, double-staining was performed as described previously[11]. Briefly, sections were incubated with mouse anti-TrkC antibody (1:800; Upstate Biotechnology Inc., Lake Placid, NY, USA) at 4 °C for 24 h. After being washed for 3 times, sections were incubated with Alexa Fluor 488 goat anti-mouse secondary antibody (1:200; Molecular Probes, Eugene, OR, USA). For double-labeling, the same sections were washed for 3 times and then incubated with rabbit anti-glial fibrillary acidic protein (GFAP) antibody (Zymed Laboratory, CA, USA) for 2 h, followed by Alexa Fluor 594 goat anti-rabbit secondary antibody (1:400; Molecular Probes, Eugene, OR, USA) for 1 h at 37 °C. The sections were observed under inverted microscope (Leica DMIRE2, Germany). Green color indicated TrkC immunoreactive (IR) staining, and red color indicated GFAP IR staining. Cell nucleus with 4',6-diamidino-2-phenylindole (DAPI) staining exhibited blue color. Negative controls omitting the primary antibody showed negative results.

2.5 *In situ* hybridization *In situ* hybridization was performed as previously described[11]. Briefly, tissues were treated with 4% paraformaldehyde followed by proteinase K (20 mg/mL), and then incubated in 0.1 mol/L triethanolamine with acetic anhydride. Following dehydration, tissues were hybridized with antisense cRNA probes (25 000 cpm/mL) in a buffer containing 13×Denhardt's solution, 0.3 mol/L NaCl, 20 mmol/L Tris-Cl (pH 7.4), 10 mmol/L DTT, 50% formamide, and 0.5 mg/mL yeast tRNA at 55 °C for 16–20 h. After hybridization, tissues were washed with 43 SSC and 10 mmol/L DTT at 50 °C. Slides were incubated with RNase A (20 mg/mL) and RNase T1 (2 mg/mL) at 37 °C for 45 min, followed by 2-h wash in 50% formamide, 0.23 SSC, and 10 mmol/L DTT at 65 °C. Finally, slides were washed twice in 0.23 SSC and 10 mmol/L DTT, and then dehydrated in a graded series of ethanol. The slides were dipped in emulsion (Kodak NTB-2) and exposed for 5–10 d at 4 °C. The slides were developed in Kodak D-19 solution, fixed, and coverslipped. Tissues were visualized and photographed with dark field using an Olympus BX50 microscope.

2.6 Western blot Briefly, cells were washed in 1 mol/L PBS and lysed in RIPA buffer (Roche, Mannheim, Germany). Protein concentrations were determined using the Bradford method. For electrophoresis, protein samples (50 μg each) were dissolved in sample buffer (60 mmol/L Tris-HCl, pH 6.8, 14.4 mmol/L β-mercaptoethanol, 25% glycerol, 2% SDS, and 0.1% bromophenol blue), and heated at 100 °C for 5 min. Samples were then resolved on 10% SDS-PAGE and transferred to PVDF membranes (Bio-Rad, Hercules, USA). The membranes were blocked in PBS containing 5% non-fat dry milk for 1 h, followed by incubation with mouse anti-TrkC (1:400; Upstate Biotechnology, NY, USA) at 4 °C overnight. After being washed, the membranes were incubated with peroxidase-conjugated goat anti-mouse IgG (1:50 000; Golden Bridge Biotechnology, Beijing, China). Proteins were visualized by ECL Chemiluminescence (Sigma, Santa Clara, USA). All western blot experiments were repeated for at least 3 times. β-Actin served as an internal control.

2.7 Real time RT-PCR Total cellular RNA was extracted from T9–T12 spinal segments by using RNAeasy total RNA purification kit (QIAGEN, Hilden, Germany), followed by treatment with RNase-free DNase (QIAGEN, Hilden, Germany). Quantitative real-time one-step RT-PCR was carried out by using the LightCycler System (Roche, Mannheim, Germany), and amplification was monitored and analyzed by measuring the binding of the fluorescence dye SYBR green I to double-stranded DNA. One microliter of total RNA was reversely transcribed and subsequently amplified by using QuantiTect SYBR green RT-PCR Master mix (QIAGEN, Hilden, Germany) and 0.5 μmol/L of both sense and antisense primers. After amplification, melting curves of the RT-PCR products were acquired, demonstrating the product specificity. The primers of *TrkC* gene were as follows: forward GGATTCAGG-

GAACAGCAATGGG, reverse GCAAAGGAGAGCCAGAGCCATT. Glyceraldehyde-3-phosphate dehydrogenase (GAPDH) was used as an endogenous control to normalize expression level of *TrkC* gene.

2.8 Data analysis All results were expressed as means± SEM. The statistical significance of differences between groups was determined by one-way analysis of variance (ANOVA) followed by Tukey's *post hoc* multiple comparison tests. $P < 0.05$ was considered as statistically significant. Each experiment consisted of at least 3 replicates per condition. Statistical analyses were performed using SPSS version 12.0 (Chicago, IL, USA).

3 Results

3.1 Expression of TrkC in the normal and the injured spinal cords and in cerebral cortex In the normal spinal cord, TrkC IR products were found in motoneurons and most other neurons in the gray matter (Fig. 1A, B). Some astrocytes as identified by GFAP antibody within the white matter were also TrkC-positive (Fig. 1C). However, TrkC IR products were not detected in the precentral gyrus of cerebral cortex (Fig. 1D). Immunohistochemical control was used to detect specificity of the antisera. No specific staining was present when the primary antibody was omitted (Fig. 1E) or preabsorbed with TrkC (Fig. 1F).

In the ventral spinal motoneurons of normal spinal cord, TrkC IR was localized mainly in the cytoplasm of cells, but hardly in the dendritic processes or nerve terminals (Fig. 1G). However, at 14 dpo, the nuclei staining of TrkC was enhanced markedly, and the intense staining of TrkC was also observed in some dendritic arborizations and axons (Fig. 1H). TrkC IR products were not detected in the motor cortex after injury.

By using *in situ* hybridization, *TrkC* mRNA signals were detected in the ventral horn of both normal (Fig. 1I) and injured (Fig. 1J) spinal cord. However, at 14 d post injury, the signal intensity in the ventral horn was obviously down-regulated, as compared with that in normal rats. In the white matter of both control and injured spinal cords, *TrkC* mRNA expression was below the detection level.

3.2 Temporal changes in the levels of TrkC protein and mRNA in the spinal cord and motor cortex As shown in Fig. 2A and B, TrkC protein levels in the epicenter of the injury site (T10–T11) and the neighboring spinal segments (T9 and T12) were down-regulated at 1, 3 and 7 dpo, as compared with those in sham-operation group. However, the level of TrkC recovered to the sham level at 14 dpo. In comparison, TrkC protein level was significantly higher in the rostral stumps than in the caudal stumps. Besides, TrkC protein level was significantly higher in the epicenter of the injury site than in the neighboring spinal segments. TrkC protein was not detected in the precentral gyrus of cerebral cortex by western blot.

The temporal change in the level of *TrkC* mRNA showed a similar change pattern with that of TrkC protein after injury (Fig. 2C–E). The level of *TrkC* mRNA was sharply decreased at 1, 3 and 7 dpo, when compared with sham-operation group, but it recovered to a level higher than the sham level at 14 dpo. The level of *TrkC* mRNA in the precentral gyrus of cerebral cortex remained relatively lower at different time points compared with the sham level.

4 Discussion

Under normal conditions, TrkC IR was widely observed in pyramidal-like motoneurons and stellate-like interneurons in the spinal ventral horn, but not in the cerebral cortex, which is consistent with the previous findings[12,13]. These results imply that TrkC plays a role in the normal physiological processes of motor neurons. In addition, TrkC was found to be widely distributed in the neurons of intermediate zone and dorsal horn and in astrocytes in the spinal cord of rat. These cells could be the potential sources of TrkC in the spinal cord.

In the present study, *TrkC* mRNA expression was found to be down-regulated in the earlier stage after injury (3–7 dpo), but up-regulated in the later stage after injury (14 dpo). This is somewhat different from a recent report by Hajebrahimi *et al*.[14] who revealed that *TrkC* mRNA expression is continuously down-regulated and completely shut down in the injured cord up to 3 weeks after contusive injury. This discrepancy may be attributed to the differences in animal models and in the experiment methods

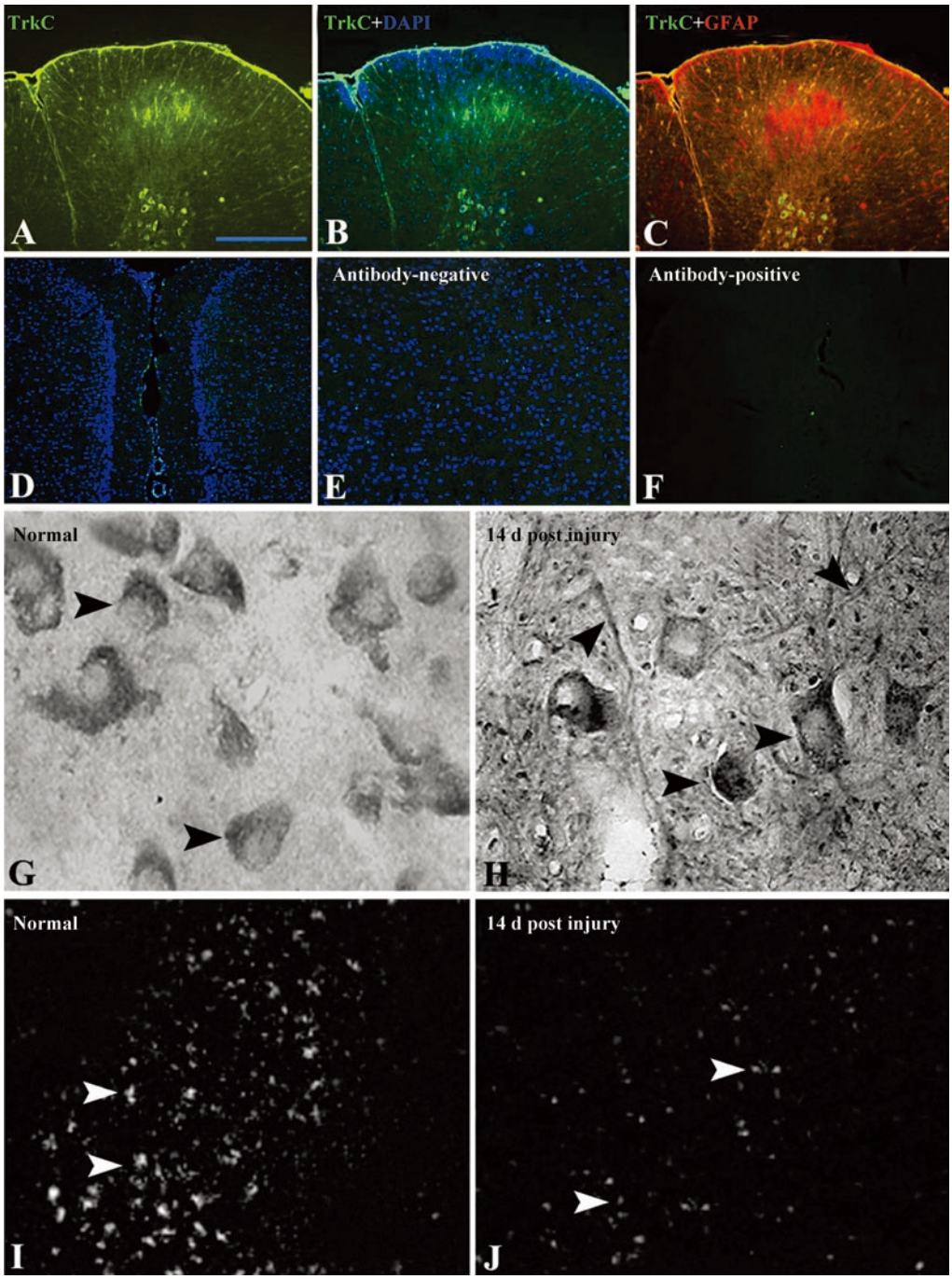

Fig. 1 **A,B: TrkC immunoreactive (IR) staining in the ventral horn of normal spinal cord. C: The double staining for TrkC and GFAP in the normal spinal cord. D: No TrkC IR staining was observed in the precentral gyrus of the motor cortex. No specific staining was observed when the anti-TrkC antibody was omitted (E) or preabsorbed with TrkC (F). G: In the ventral spinal motoneurons of normal spinal cord, TrkC IR was localized mainly in the cytoplasm of cells, as shown by the arrowheads. H: The TrkC staining was enhanced in the nuclei at day 14 after injury. The TrkC staining was also observed in the dendritic arborizations and axons, as shown by the arrowheads. I, J: *TrkC* mRNA signals were detected in the ventral horns of both normal (I) and injured (J) spinal cords, as revealed by *in situ* hybridization. However, in comparison with that in normal spinal cord, the signal intensity was obviously down-regulated in injured spinal cord at 14 dpo. Scale bar for A–D and F, 200 μm. Scale bar for E, 75 μm. Scale bar for G and H, 25 μm. Scale bar for I and J, 50 μm.**

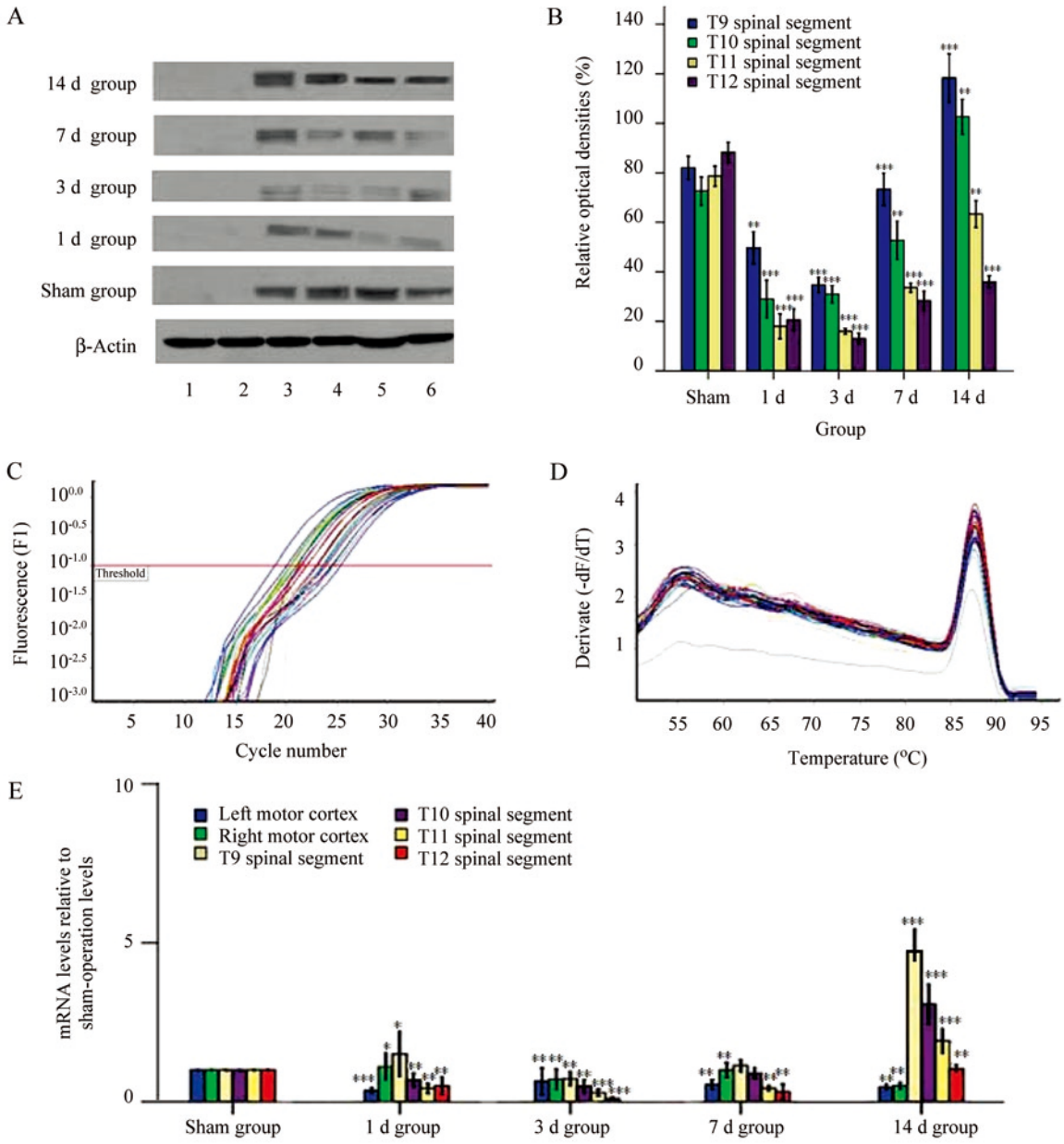

Fig. 2 A: Western blot results of TrkC protein levels in the spinal segments and in precentral gyrus of cerebral cortex at 1, 3, 7, and 14 d post injury. Lane 1: left precentral gyrus; lane 2: right precentral gyrus; lane 3: T9 spinal segment; lane 4: T10 spinal segment; lane 5: T11 spinal segment; lane 6: T12 spinal segment. B: Semi-quantification of TrkC protein level by optic density analysis of the bands. C: Representative real-time RT-PCR analysis using the LightCycler® technique. Plot of the fluorescence versus the cycle number obtained from SYBR Green detection of serially diluted FN1 mRNA (encoding fibronectin) (left). The horizontal line represented the position of the threshold. D: Melting curve analysis showed the specificity of PCR products. E: Quantification of *TrkC* mRNA level by real-time PCR. $^{**}P < 0.01$, $^{***}P < 0.001$ *vs* sham-operation control group.

employed, because complete transection can lead to severe damage of the spinal cord which is restricted to the level of injury, whereas contusive injury may induce egg-shaped zone of necrosis that extends through several spinal cord segments rostrocaudally[15]. One important difference between the 2 injury models is that in weight-drop injuries, the dura is left mechanically intact, whereas in the transection model, the dura is cut, exposing the spinal cord. Cut-

ting the dura has severe consequences for the cerebrospinal flow and may aggravate secondary degenerative processes. In fact, the transection injury is not a good model to mimic human SCI because compression plays a significant role in the development of secondary injury. However, the complete transection could avoid function repair mediated by the spare axons in the incomplete animal models. Thus, for the present study, the complete transection model serves better to explore the reparation mechanisms. On the other hand, our results are consistent with several previous reports[15,16]. Furthermore, here the temporal change pattern of TrkC protein level demonstrated by immunohistochemical staining and western blot is consistent with that of *TrkC* mRNA expression examined by RT-PCR.

The down-regulation of TrkC level may result from both motoneuron death and loss of TrkC transport after axotomy in the cord transection. It may also be attributed to the subsequent activations of various noxious and destructive pathophysiological processes. For the up-regulation of TrkC level in the latter stage after injury (14 dpo), several factors may be responsible for this change, including induction of *de novo* synthesis of NTs by neurons and/or glial cells[17], invasion of activated inflammatory cells and oligodendrocytes that can express TrkC as demonstrated in earlier studies[12,13]. Besides, the endogenous repair system will be enhanced after SCI, such as up-regulation of TrkC in the caudal stump of spinal cord. The up-regulated TrkC interacts with NT-3 to attract axotomized fibers to extend, and re-enter the caudal and the rostral part of the spinal cord, thereby promoting spinal cord regeneration. Interestingly, our previous studies[7] revealed that the number of NT-3-positive neurons and the OD value of NT-3 increase dramatically from days 3–21 after spinal transection in adult rats, compared with sham-operation group. However, the functional recovery is not apparent at the earlier stage after injury. This can probably be explained that despite the increase in NT-3 level, TrkC, the receptor of NT-3, has a low level and fails to mediate the respective trophic activities of NT-3. Therefore, exogenous administration of TrkC at this stage may possibly improve the locomotor functional recovery, which needs to be verified in our future studies.

The absence of TrkC protein in the pyramidal layer of motor cortex was demonstrated in the present study. Hence, anterograde transportation of NT-3 protein from motor cortex seems not to be a potential source of NT-3 in the spinal cord. The protein and mRNA levels of TrkC showed the same change patterns following injury, indicating that *in situ* synthesis by spinal motoneurons themselves constitutes a major source of TrkC. In addition, TrkC levels in the nearest caudal and rostral segments at the site of transection were significantly higher than those in the neighboring segments, probably due to the blockade of TrkC transportation and the resulting protein accumulation on either side of the epicenter[17]. In comparison, TrkC protein and mRNA levels in the rostral segment recovered to be higher than those in the caudal segment. TrkC accumulation around the site of injury can transduce NT-3 signals, and NT-3 may have a positive effect on axonal regeneration from proximal site of the injured axons, which is known to occur in the condition of sciatic nerve injury[17,18]. It has been widely reported that regeneration of axons in the rostral stumps is stronger than that in the caudal stumps. The enhanced transportation of TrkC protein through axonal pathways may improve TrkC level in the rostral stumps.

In conclusion, the results of the present study provide novel and suggestive evidence supporting that TrkC plays an important role in the spinal cord during development and after injury, and raise the importance of the correlated receptors of NTs, apart from NTs themselves.

Acknowledgements: This work was supported by the grants from National Natural Science Foundation of China (No. U0632008), the Key Project of Science and Technology Research Foundation of Guangdong Province, China (No. 2008A030201019, 2007-05/06-7005206), the Key Project of Science and Technology Research Foundation of Guangzhou municipality, China (No. 09B52120112, 2008A1-E4011-6), and the Foundation for Medical and Scientific Technology Research of Guangdong Province, China (No. A2009293).

References:

[1] Markus A, Patel TD, Snider WD. Neurotrophic factors and axonal growth. Curr Opin Neurobiol 2002, 12: 523–531.

[2] Grill R, Murai K, Blesch A, Gage FH, Tuszynski MH. Cellular delivery of neurotrophin-3 promotes corticospinal axonal growth and partial functional recovery after spinal cord injury. J Neurosci 1997, 17: 5560–5572.

[3] Scott AL, Borisoff JF, Ramer MS. Deafferentation and neurotrophin-mediated intraspinal sprouting: a central role for the p75 neurotrophin receptor. Eur J Neurosci 2005, 21: 81–92.

[4] Zhou L, Shine HD. Neurotrophic factors expressed in both cortex and spinal cord induce axonal plasticity after spinal cord injury. J Neurosci Res 2003, 74: 221–226.

[5] Zhang HT, Gao ZY, Chen YZ, Wang TH. Temporal changes in the level of neurotrophins in the spinal cord and associated precentral gyrus following spinal hemisection in adult Rhesus monkeys. J Chem Neuroanat 2008, 36: 138–143.

[6] Kawakami H, Nitta A, Matsuyama Y, Kamiya M, Satake K, Sato K, *et al.* Increase in neurotrophin-3 expression followed by Purkinje cell degeneration in the adult rat cerebellum after spinal cord transection. J Neurosci Res 2000, 62: 668–674.

[7] Zhang HT, Li LY, Zou XL, Song XB, Hu YL, Feng ZT, *et al.* Immunohistochemical distribution of NGF, BDNF, NT-3, and NT-4 in adult rhesus monkey brains. J Histochem Cytochem 2007, 55: 1–19.

[8] Li XL, Zhang W, Zhou X, Wang XY, Zhang HT, Qin DX, *et al.* Temporal changes in the expression of some neurotrophins in spinal cord transected adult rats. Neuropeptides 2007, 41: 135–143.

[9] Qin DX, Zou XL, Luo W, Zhang W, Zhang HT, Li XL, *et al.* Expression of some neurotrophins in the spinal motoneurons after cord hemisection in adult rats. Neurosci Lett 2006, 410: 222–227.

[10] Zhang HT, Cheng HY, Zhang L, Fan J, Chen YZ, Jiang XD, *et al.* Umbilical cord blood cell-derived neurospheres differentiate into Schwann-like cells. Neuroreport 2009, 20: 354–359.

[11] Kordower JH, Chen EY, Sladek JR Jr, Mufson EJ. trk-immunoreactivity in the monkey central nervous system: forebrain. J Comp Neurol 1994, 349: 20–35.

[12] Sandell JH, Baker LS Jr, Davidov T. The distribution of neurotrophin receptor TrkC-like immunoreactive fibers and varicosities in the rhesus monkey brain. Neuroscience 1998, 86: 1181–1194.

[13] Duberley RM, Johnson IP, Anand P, Leigh PN, Cairns NJ. Neurotrophin-3-like immunoreactivity and Trk C expression in human spinal motoneurones in amyotrophic lateral sclerosis. J Neurol Sci 1997, 148: 33–40.

[14] Hajebrahimi Z, Mowla SJ, Movahedin M, Tavallaei M. Gene expression alterations of neurotrophins, their receptors and prohormone convertases in a rat model of spinal cord contusion. Neurosci Lett 2008, 441: 261–266.

[15] Widenfalk J, Lundstromer K, Jubran M, Brene S, Olson L. Neurotrophic factors and receptors in the immature and adult spinal cord after mechanical injury or kainic acid. J Neurosci 2001, 21: 3457–3475.

[16] Liebl DJ, Huang W, Young W, Parada LF. Regulation of Trk receptors following contusion of the rat spinal cord. Exp Neurol 2001, 167: 15–26.

[17] Murakami Y, Furukawa S, Nitta A, Furukawa Y. Accumulation of nerve growth factor protein at both rostral and caudal stumps in the transected rat spinal cord. J Neurol Sci 2002, 198: 63–69.

[18] Heumann R, Korsching S, Bandtlow C, Thoenen H. Changes of nerve growth factor synthesis in nonneuronal cells in response to sciatic nerve transection. J Cell Biol 1987, 104: 1623–1631.

成年大鼠脊髓全横断损伤后酪氨酸激酶受体 C 在脊髓和大脑皮层的表达

钱东翔[1,2]，张洪钿[2,3]，蔡颖谦[2]，罗鹏[1]，徐如祥[2,3]

[1] 广州医学院第三附属医院神经外科，广州 510150；[2] 广东省脑功能修复与再生重点实验室，广东神经外科研究所，南方医科大学，广州 510282；[3] 中国人民解放军北京军区总医院神经外科，北京 100700

摘要：目的 研究神经营养因子3(neurotrophin-3, NT-3)的受体—酪氨酸激酶受体C(tyrosine kinase receptor C, TrkC)在脊髓损伤(spinal cord injury, SCI)后神经重塑中的作用。**方法** 研究脊髓全横断损伤大鼠手术后第1、3、7和14 d时，低位胸髓节段和大脑中央前回TrkC的表达。**结果** 损伤节段(T10–T11)双侧和临近节段(T9和T12)的TrkC蛋白水平在术后1–7 d显著下调，而在术后14 d快速增强。此外，*TrkC* mRNA表达水平的暂时性变化与TrkC蛋白的变化模式相似。TrkC蛋白和mRNA在损伤节段(T10–T11)的水平显著高于在临近节段(T9和T12)的水平。此外，TrkC蛋白和mRNA在吻侧节段的水平高于在尾侧节段的水平。与脊髓不同的是，运动皮层中并未检测到TrkC蛋白，并且*TrkC* mRNA的表达水平也很低。**结论** TrkC可能与脊髓损伤后的神经功能重塑有关。

关键词：酪氨酸激酶受体C；脊髓损伤；可塑性；mRNA